Lava volume from the 1997 Eruption of Okmok volcano, Alaska, estimated using spaceborne and airborne interferometric synthetic aperture radar

Zhong Lu, U.S. Geological Survey, EROS Data Center, Raytheon ITSS, Sioux Falls, SD 57198; Phone: 605-594-6063, Fax: 605-594-6529, Email: lu@usgs.gov

Matt Patrick, Alaska Volcano Observatory, Geophysical Institute, University of Alaska, Fairbanks, AK 99775; Phone: 907-474-6839, Fax: 907-474-7290, Email: patrick@gi.alaska.edu

Eric Fielding, Jet Propulsion Laboratory, 4800 Oak Grove Drive, Pasadena, CA 91109. Phone: 818-354-9305, Fax: 818-354-9476, Email: Eric.Fielding@jpl.nasa.gov

Charles Trautwein, U.S. Geological Survey, EROS Data Center, Sioux Falls, SD 57198; Phone: 605-594-6015, Fax: 605-594-6529, Email: trautwein@usgs.gov

ABSTRACT

Interferometric synthetic aperture radar (InSAR) techniques are used to calculate the volume of eruption at Okmok volcano, Alaska by constructing precise digital elevation models (DEMs) that represent volcano topography before and after the eruption. The pre-eruption DEM is generated using TOPSAR data where a three-dimensional multi-affined transformation is used to account for the misalignments between different DEM patches. The post-eruption DEM is produced using repeat-pass ERS data; multiple interferograms are required to reduce errors due to atmospheric contribution. The eruption volume associated with the 1997 eruption of Okmok volcano is 0.165±0.028 km^3. The thickest portion is ~50 m, although field measurements of the flow margin's height don't exceed 20 m. Therefore, the in-situ measurements at lava edges are not representative of total thickness and precise DEM data are absolutely essential to calculate eruption volume based on lava thickness estimations. This is an example that demonstrates how InSAR will play a significant role on studying arctic volcanoes.

INTRODUCTION

Estimating eruption volume is a critical component of volcanology. Accurate mapping of the erupted material is valuable for constraining magma supply and understanding magma plumbing system [e.g., Wadge 1977; Crisp 1984; Dvorak and Dzurisin, 1993; Rowland et al., 1999]. Calculating eruption volume requires accurate mapping of the pre- and post-eruption digital elevation models (DEMs). In the absence of high-precision DEMs, the eruptive volume is often calculated by multiplying the extent of new lava and the average thickness of the eruptive material, estimated at several points along the lava edges. Therefore accurate calculation of the eruptive volume has been generally not feasible. For Alaska volcanoes, the remote locations, difficult logistics, and persistent

cloud cover hinder the precise mapping of high resolution DEMs obtained using optical photogrammetry or LIDAR techniques [Molander, 2001; Fowler, 2001].

Interferometric synthetic aperture radar (InSAR) has proven the great potential of producing detailed DEMs over a large area [e.g., Hensley et al., 2001; Massonnet and Feigl, 1998; Rosen et al., 2000; Zebker et al., 2000]. Synthetic aperture radar (SAR) is an active system that both transmits microwave signals and receives the backscattered signals from the Earth's surface. Radar signals can penetrate through the atmosphere to the ground surface in virtually all types of weather, day or night. InSAR is formed by interfering signals from two spatially separated antennas. The separation of the two antennas is called the baseline. The two antennas may be mounted on a singe platform, the usual implementation for aircraft and spaceborne systems such as TOPSAR and SRTM missions [e.g., Zebker et al., 1992; Farr and Kobrick, 2001]. Alternatively, InSAR can be created by utilizing a single antenna on an airborne or spaceborne platform in nearly identical repeating orbits [e.g., Massonnet and Feigl, 1998]. For the latter case, even though the antennas do not illuminate the same area at the same time, the two sets of signals recorded during the two passes will be highly correlated if the scattering of the ground surface is unchanged between viewings. This is the typical implementation for spaceborne sensors such as the European Remote-sensing Satellite (ERS-1/-2), Canadian Radar Satellite (Radarsat-1), and Japanese Earth Resource Satellite (JERS-1), which operate at wavelengths ranging from a few centimeters (C-band) to tens of centimeters (L-band). InSAR has proven capable of mapping ground deformation with centimeter-scale precision and producing accurate DEMs with several meters accuracy [e.g., Hensley et al., 2001; Massonnet and Feigl, 1998; Rosen et al., 2000; Zebker et al., 2000].

In this paper, we use InSAR derived DEMs to estimate the eruption volume of Okmok volcano, Alaska, which last erupted in 1997 (Figure 1). Okmok volcano, a broad shield topped with a 10-km-wide caldera, occupies most of the northeastern end of Umnak Island, Alaska (Figure 1). The caldera was formed more than 2400 years ago [Byers, 1959]. Eruptions in this century happened in 1931, 1936, 1938, 1943, 1945, 1958, 1960, 1981, 1983, 1986, 1988, and 1997 [Miller et al., 1998]. All historic eruptions of Okmok originated from Cone A, a cinder cone located on the southern edge of the caldera floor. Abundant ash emissions and mafic lava flows originating from Cone A have crossed the caldera floor. The latest eruption of Okmok volcano began in early February 1997 and ended in late April 1997. The eruption was a moderate strombolian type with an ash plume reaching to 10,000 m. ERS-1/-2 InSAR data were used to map the pre-eruptive, co-eruptive, and post-eruptive deformation [Lu et al., 1998, 2000]. The authors measured about 140 cm of subsidence associated with the 1997 eruption of Okmok volcano. This subsidence occurred during an interval beginning 16 months prior to the eruption and ending 5 months after the eruption. The subsidence was preceded by about 18 cm of uplift, centered in the same location, between 1992 and 1995, and was followed by about 10 cm of uplift between September 1997 and 1998 [Lu et al., 2000].

To estimate the eruption volume from 1997 eruption at Okmok volcano, we use two precise DEMs best describing the volcano topography before and after the 1997 eruption. The post-eruption DEM is produced using airborne (TOPSAR) InSAR system while the

pre-eruption DEM is generated using spaceborne (ERS-1/ERS-2) repeat-pass InSAR data. We first discuss the background of InSAR DEM generation. Then we present the procedure for producing the DEM mosaic from TOPSAR data and the procedure for generating the DEM from repeat-pass ERS-1/ERS-2 data. Finally, eruption volume associated with 1997 eruption of Okmok volcano is calculated.

BACKGROUND OF INSAR DEM GENERATION

The theory of DEM generation by the means of InSAR has been addressed in many papers [e.g., Hensley et al., 2001; Massonnet and Feigl, 1998; Rosen et al., 2000; Sansosti, et al., 1999; Zebker et al., 2000]. Here, we just review the particular issues affecting DEM accuracy.

Firstly, a major error source in InSAR DEM generation is the baseline uncertainty due to inaccurate determination of satellite positions. Errors in this value propagate into very large systematic errors of terrain height. For this study, the precision orbit data product (PRC) delivered by the German Processing and Archiving Facility (D-PAF) for ERS-1/ERS-2 satellites [Massmann, 1995] is used to improve the baseline vector estimation. PRC state vectors are given at 30-second intervals. The accuracy of the PRC position vectors is approximately 30 cm for along-track and 8 cm for cross-track [Massmann, 1995]. The ERS interferometric baseline estimation is further improved by using ground control points (GCP) [e.g., Rosen et al., 1996]. For the TOPSAR data, due to precise the navigation systems on the aircraft and fixed baseline length [Zebker et al, 1992], further refinement is not necessary for baseline determination.

Secondly, because the phase of radar signal is used to estimate elevation, error in phase measurement also contributes to the topographic error. The phase error is generally caused by the thermal noise in the SAR system and environmental change of the imaged surface. The elevation error due to phase error is inversely proportional to the perpendicular component of baseline length; longer baselines are necessary for high-precision DEMs. However, longer baselines cause more decorrelation, which increases the phase error and consequently the elevation error. Therefore we choose interferograms with the largest available baseline within the limits of correlation [e.g., Rodriguez and Martin, 1992; Zebker et al., 1997].

Thirdly, a critical error source in InSAR-derived DEM is due to atmospheric delay anomalies caused by small variations in the index of refraction along the line of propagation [e.g., Zebker et al., 1997]. Changes in the total electron content of the ionosphere and turbulance in the troposphere will result in variations of phase of signals, which will introduce errors in the observed interferogram. Height errors due to atmospheric anomalies are typically not as large as those resulting from baseline errors, but less systematic [e.g., Goldstein 1997; Zebker et al., 1997]. In order to produce an accurate DEM from ERS data, it is therefore required 1) to choose interferograms with relatively long baselines as the effect of atmospheric anomalies on DEM is inversely proportional to baseline length, and 2) to average multiple interferograms to reduce the atmospheric effects [e.g., Zebker et al., 1997].

Finally, we must take into account any possible surface deformation due to tectonic loading sources, over the time interval spanned by the interferogram. Therefore, interferograms with shorter temporal separation are preferred for generating DEMs. The ERS-1/ERS-2 tandem data will meet this requirement in most cases. So-called tandem pairs are acquired by adjusting the ERS-1 and ERS-2 orbits, both of which repeat every 35 days, to follow one another by 1 day. Thus, a point on the surface is imaged by one satellite (ERS-1) on a given day and by the other satellite (ERS-2) on the following day. In the case where tandem data are not available or not appropriate for DEM generation, deformation rates should be estimated independently and removed from the interferograms used for DEM production.

POST-ERUPTION DEM: TOPSAR DEM PROCESSING

TOPSAR is a left-looking, two-antenna InSAR system onboard a NASA DC-8 aircraft. The baseline of the two antennas is 2.5 m, oriented about 27.2° from the vertical [Zebker et al., 1992; Madsen et al., 1995]. The normal altitude of the aircraft is about 9 km, and the radar look angles range between 30° and 55° from the vertical. Because the two interferometric images are acquired simultaneously, atmospheric effects do not play a role in TOPSAR DEM generation. The TOPSAR data presented here are collected at 40 MHz C-band (wavelength of 5.7 cm). Image swath width in range direction is about 10 km, and slant range resolution is about 3.3 m. The derived DEM has a pixel spacing of 5 m and RMS height error of about 1-3 m [Zebker et al., 1992; Madsen et al., 1995].

Ten flight passes were made over the Okmok volcano during the 2000 Pacific Rim Campaign (http://airsar.jpl.nasa.gov). We have obtained 10 DEMs, each of which corresponds to an individual flight pass, from the Jet Propulsion Laboratory (JPL). Flight heading angles are 53° for 4 passes, 233° for 3 passes, 324° for 2 passes, and 144° for 1 pass. A DEM mosaic was produced based on metadata provided in each DEM. Visual checking suggests that height offsets between two DEMs with overlap are far larger than the specified vertical accuracy of ~3 m. Hence, geometric correction procedures are needed to render a DEM mosaic with vertical accuracy consistent with the TOPSAR specification.

To account for the horizontal and vertical mis-alignments between different TOPSAR passes, we used the multi-affined transformation approach proposed by JPL [see Chapin, 2000]. The basic concept is to fully utilize the three-dimensional shifts (both the horizontal and vertical ones) calculated between any two TOPSAR passes with overlap. Treating each pixel in the TOPSAR DEM imagery as a three-dimensional vector, the following transformation is used to convert the input vector, I, into a output vector, O [Chapin, 2000]:

$$O = MI + T$$

$$M = \begin{bmatrix} Lx & 0 & 0 \\ 0 & Ly & 0 \\ 0 & 0 & Lz \end{bmatrix} + Qx \begin{bmatrix} 0 & 0 & 0 \\ 0 & 0 & -1 \\ 0 & 1 & 0 \end{bmatrix} + Qy \begin{bmatrix} 0 & 0 & 1 \\ 0 & 0 & 0 \\ -1 & 0 & 0 \end{bmatrix} + Qz \begin{bmatrix} 0 & -1 & 0 \\ -1 & 0 & 0 \\ 0 & 0 & 0 \end{bmatrix}$$

$$T = \begin{bmatrix} Tx & Ty & Tz \end{bmatrix}^T$$

Where, M is the transformation matrix; Lx, Ly, and Lz are scale factors in x, y, and z directions; Qx, Qy, and Qz are the factors of rotation about the x, y, and z axes. T is the translation vector with its components Tx, Ty, and Tz. The offset estimations, used for calculating the 3-D multi-affined transformation matrix M and the translation vector T, are obtained by cross-correlation technique based on both radar amplitude images and the corresponding DEM images. It is suggested to use amplitude images for parallel and antiparallel passes, and to use DEM images for scenes that cross at any other angle [Chapin, 2000]. For the 10 TOPSAR passes over the Okmok volcano, we produced 19 sets of offset estimates. These offsets were furthered refined to remove outliers. We find that normal horizontal offsets between different passes are less than 15 m. However, one particular scene is offset from others by about 50 m. The TOPSAR DEM mosaic, refined with the three-dimensional multi-affined transformation technique, is shown in Figure 1.

Figure 2a shows the difference of two DEM mosaics produced with and without the multi-affined transformation. The height difference along the profile AB is shown in Figure 2b. Height difference ranges from –25 m to 40 m, and is caused by both horizontal and vertical misalignments between individual DEMs used to produce the DEM mosaic.

PRE-ERUPTION DEM: ERS INSAR DEM PROCESSING

Repeat-pass ERS-1 and ERS-2 SAR images have been demonstrated capable of producing high-accuracy DEMs [e.g., Sansosti et al., 1999; Ferretti et al., 1999]. However, atmospheric anomalies need to be carefully considered because images used for InSAR processing are acquired at different times. Also, compromise between baseline and interferometric coherence has to be balanced to select InSAR pairs suitable for DEM generation. Finally, for tectonically active regions, deformation signal must be removed from the interferograms used for DEM generation.

Ground surface deformation associated with 1997 eruption at Okmok volcano has been systematically studied [Lu et al., 1998, 2000]. The reported pre-eruptive inflation is ~9 mm/month during October 31, 1992 and November 20, 1993, and ~3 mm/month [Lu et al., 2000]. In addition to the images shown in Lu et al. [2000], we produced several more image pairs with small baseline as well as short time separation (Figure 3). The first interferogram spans from June 14 to August 23, 1993, with the perpendicular component of baseline, Bn, equal to 32 m (Figure 3a). The second interferogram covers the time interval from September 11 to October 16, 1993 with B_n = 25 m (Figure 3b). The third interferogram spans the time window between May 22, and September 4, 1995 with B_n = 22 m (Figure 3c). Because these interferograms have very small baseline, they are insensitive to DEM errors. Therefore, we can use either the post-eruption TOPSAR DEM (Figure 1) or the existing DEM [Lu et al., 2000] to remove topographic effects for

deformation analysis. Because these interferograms have shorter time separation and are temporally close to the interferograms used for DEM generation, they better depict the deformation occurred over the interferograms used for DEM generation (Table 1). We estimate the deformation is about 12 mm and 8 mm per 35 days during summers of 1993 and 1995, respectively.

Among the available SAR images acquired before 1997 eruption, 4 pairs were selected for DEM generation (Table 1). In general, interferometric coherence is maintained reasonably well within the caldera and it is lost around the caldera rim where terrain is rugged and persistent snow patches are present. This is sufficient as we only intend to produce a pre-eruption topographic height within the caldera floor, part of which is covered by the new lava from the 1997 eruption.

The baseline vectors for all the interferograms are calculated using PRC vectors from D-PAF [Massmann, 1995]. These baseline vectors are further refined using the post-eruption DEM from the above-mentioned TOPSAR data based on the approach proposed by Rosen et al. [1996] and ground control points (GCP) from the TOPSAR DEM mosaic (Figure 1). About 1000 GCPs are selected, and all of them lie within the caldera but far away from the 1997 lava flows. Because the precision restitute vectors are used, the refined baseline is not very much different from the one without GCPs.

An unwrapped interferometric phase together with the precision baseline and imaging geometry are needed to derive the topographic heights [e.g., Hensley et al., 2001]. The following hierarchy approach is used to facilitate the phase unwrapping procedure [Goldstein et al., 1988; Costantini, 1998]. We start with the interferogram with smallest baseline (i.e., the tandem pair acquired on October 25 and 26, 1995). We first subtract the topographic phase from the interferogram (also called earth-flattening) using the TOPSAR DEM. The residual fringes are unwrapped (Figure 4a), and the topographic phase is added back to this result. A DEM based on this tandem interferogram is then produced. Next, we unwrap the Aug-Sep 1993 interferogram with B_n = 403 m (Table 1), because the coherence for this interferogram is better than the Oct-Nov 1993 pair (with B_n = 395 m) (Table 1). The simulated topographic phase based on the TOPSAR DEM is removed from the interferogram. The resulting residual interferogram is unwrapped [Costantini, 1998] (Figure 4b), and a DEM is generated. Note that we did not use the DEM from the tandem interferogram to simulate the topographic phase, because the TOPSAR DEM is far more accurate than the DEM based on the tandem pair. The tandem DEM is produced from an interferogram with a small baseline. Consequently, the interferometric phase is not very sensitive to topographic relief and any possible atmospheric delay anomalies in the data will bias significantly the DEM accuracy. However, if an existing DEM is not available, the DEM produced using the interferogram with smaller baseline will be used to simulate the topographic phase in the interferogram with larger baseline. Finally, the DEM produced using the interferogram with B_n = 403 m (Figure 4b) is then used to assist unwrapping the Oct-Nov 1993 pair (with B_n = 395 m) (Figure 4c) and the interferogram with B_n = 690 m (Figure 4d). Two more DEMs are produced.

A simple weighted approach is used to combine the four DEMs:

$$h = \frac{\sum_{i=1}^{4} h_i c_i B_i^2}{\sum_{i=1}^{4} c_i B_i^2} \qquad (1)$$

Where, h_i and c_i are height and coherence values from the four DEMs, B_i is the perpendicular component of the baseline for each interferogram. This equation states that the height value of each pixel in the final DEM results from the weighted average of the four DEMs; height from the interferogram with larger baseline and higher coherence will be weighed more. This procedure not only reduces the possible atmosphere-induced errors in each DEM but also improves accuracy of the final DEM. By using this procedure, a DEM depicting the topography of Okmok volcano before the 1997 eruption is finally generated.

ERUPTION VOLUME ESTIMATION

Figure 5 shows the thickness of the 1997 lava flows. The image is the difference of the pre-eruption DEM produced using ERS interferograms and the post-eruption DEM produced using TOPSAR data. The white dotted line represent the lava perimeter based on field data that were collected in August 2001 [Moxey et al., 2001]. The horizontal extent of the lava flows estimated based on a Landsat-7 ETM+ image is about 7.6 km^2. Examining Figure 5, we can see that the thickness of the lava is very heterogeneous. The thickest portion of the lava happens to be over the right arm of the Y-shaped flows, and reaches almost 50 m. The flow is thickest here because the lava lobe terminated against the terrace at the base of Cone D, and was compressed to some degree (folding is present on the surface). This is coupled with the fact that there was a substantial depression at, which caused the flow pond up. In fact, this depression hides the extreme thickness in this area (~50 m) because the closest measurements of the flow margin's height do not exceed 20 m [Moxey et al., 2001]. Therefore, measurements at the edges are not representative of total thickness, and the DEM data are absolutely essential to calculate more accurate values of lava thickness and eruption volume. The lava near the eruptive vent (Cone A) is, on average, thinner than the rest, and can be as thin as a few meters as the underlying slope is quite steep near Cone A. We calculate the volume of 1997 eruption as 0.165±0.028 km^3. This volume is about 2-3 times as large as the 0.055 km^3, estimated from field based thickness measurement [Moxey et al., 2001].

The standard deviation of our measurement can be calculated using the values of DEM difference over the areas outside of the lava flows. We estimate the uncertainty of our measurement is 2.6 m. This means the DEM produced using the four interferograms has vertical accuracy of better than 5.0 m at 95% confidence limit.

CONCLUSION

Accurate DEMs can be produced using InSAR techniques with multiple interferograms. Single-pass two-antenna InSAR systems, such as TOPSAR, are the best for DEM production as long as misalignment between different DEM patches is

corrected. Repeat-pass single-antenna InSAR systems are also capable of producing accurate DEMs, but multiple interferograms are required to reduce errors due to atmospheric contributions. We estimate the eruption volume and lava thickness for 1997 eruption at Okmok volcano, by using the TOPSAR data to produce a post-eruption DEM and the ERS InSAR imagery to generate a pre-eruption DEM. The precise calculation of the eruption volume is not achievable by using field-based lava thickness measurements.

Acknowledgements. ERS-1/ERS-2 SAR images are copyright © 1993 and 1995 ESA, and provided by the NASA/ASF. This research was supported by funding from NASA (NRA-99-OES-10 RADARSAT-0025-0056), and in part by USGS contract 1434-CR-97-CN-40274. We thank E. O'Leary, S. Shaffer, and E. Chapin for helps on working with TOPSAR data, and T. Masterlark for technical reviews and comments.

REFERENCES

Chapin, E., Users guide for multimosaic: Version 1.1, JPL Technical Memorandum, 334-97-004, 2000.

Costantini, M., A novel phase unwrapping method based on network programming, IEEE Trans. on Geoscience and Remote Sensing, 36, 813-821, 1998.

Crisp, J.A., Rates of magma emplacement and volcanic output, J. Volcanol. Geotherm. Res., 20, 177-201, 1984.

Dvorak, J.J., and D. Dzurisin, Variations in magma supply rate at Kilauea Volcano, Hawaii, J. Geophys. Res., 98, 255-268, 1993.

Farr, T. and M. Kobrick, The Shuttle Radar Topography Mission, EOS Trans., 82(47), Fall Meeting, 2001.

Ferretti, A., C. Prati, and F. Rocca, Multiplebaseline InSAR DEM reconstruction: The wavelet approach, IEEE Trans. Geoscience and Remote Sensing, 37, 705-715, 1999.

Fowler, R., Topographic lidar, in Digital Elevation Model Technolgies and Applications: The DEM Users Manual, edited by D. F. Maune, Americal Society for Photogrammetry and Remote Sensing, p. 207-26, 2001.

Goldstein, R., Atmospheric limitations to repeat-track radar interferometry, Geophys. Res. Lett., 22, 2517-2520, 1997.

Goldstein, R., H. Zebker, and C. Werner, Satellite radar interferometry: Two-dimensional phase unwrapping, Radio Science, 23, 713-720, 1988.

Hensley, S., R. Munjy, and P. Rosen, Interferometric synthetic aperture radar (IFSAR), in Digital Elevation Model Technolgies and Applications: The DEM Users Manual, edited by D. F. Maune, Americal Society for Photogrammetry and Remote Sensing, p.143-206, 2001.

Lu, Z., D. Mann, and J. Freymueller, Satellite radar interferometry measures deformation at Okmok Volcano, Eos, Transactions, 79, no. 39, 461-468, 1998.

Lu, Z., D. Mann, J. Freymueller, and D. Meyer, Synthetic aperture radar interferometry of Okmok volcano, Alaska: Radar observations, J. Geophys. Res., 105, 10791-10806, 2000.

Madsen, S. J. Martin, and H. Zebker, Analysis and evaluation of the NASA/JPL TOPSAR across-track interferometric SAR system, IEEE Transactions on Geoscience and Remote Sensing, 33, 383-391, 1995.

Massmann, F. H., Information for ERS PRL/PRC Users, GeoForschungsZentrum Potsdam Technical Note, 1995.

Massonnet, D., and K. Feigl, Radar interferometry and its application to changes in the Earth's surface, Rev. Geophys., 441-500, 1998.

Miller, T.P., R.G. McGimsey, D.H. Richter, J.R. Riehle, C.J. Nye, M.E. Yount, and J.A. Dumoulin, Catalog of the historically active volcanoes of Alaska, USGS Open-File Report 98-582, 1998.

Molander, C.W., Photogrammetry, in Digital Elevation Model Technolgies and Applications: The DEM Users Manual, edited by D. F. Maune, Americal Society for Photogrammetry and Remote Sensing, p. 121-142, 2001.

Moxey, L., and others, The 1997 eruption of Okmok volcano, Alaska, a synthesis of remotely sensed data, EOS, Trans., 82(47), Fall Meeting, 2001.

Rodriguez, E., and J. Martin, Theory and design of interferometric synthetic aperture radars, Proc. IEE, 139, 147-159, 1992.

Rosen, P.A. and others, Synthetic aperture radar interferometry, Proceedings of the IEEE, 88, 333-380, 2000.

Rosen, P., S. Hensley, H. Zebker, F. H. Webb, and E. J. Fielding, Surface deformation and coherence measurements of Kilauea volcano, Hawaii, from SIR-C radar interferometry, J. Geophys. Res., 101, 23109-23125, 1996.

Rowland, S.K., M.E. MacKay, H. Garbeil, and P.J. Mouginis-Mark, Topographic analyses of Kilauea Volcano, Hawaii, from interferometric airborne radar, Bull. Volcanol, 61, 1-14, 1999.

Sansosti, E., R. Lanari, G. Fornaro, G. Franceschetti, M. Tesauro, G. Puglisi, and M. Coltelli, Digital elevation model generation using ascending and descending ERS-1/ERS-2 tandem data, Int. J. Remote Sensing, 20, 1527-1547, 1999.

Wadge, G., The storage and release of magma on Mount Etna, J. Volcanol. Geotherm. Res., 2, 361-384, 1977.

Zebker, H.A., and others, The TOPSAR interferometric radar topographicmapping instrument, IEEE Transactions on Geoscience and Remote Sensing, 30, 933-940, 1992.

Zebker, H., P. Rosen, and S. Hensley, Atmospheric effects in interferometric synthetic aperture radar surface deformation and topographic maps, J. Geophys. Res., 102, 7547-7563, 1997.

Zebker, H., F. Amelung, and S. Jonsson, Remote sensing of volcano surface and internal processing using radar interferometry, Remote Sensing of Active Volcanism, AGU Monograph, ed.: P. Mougins-Mark et al., 179-205, 2000.

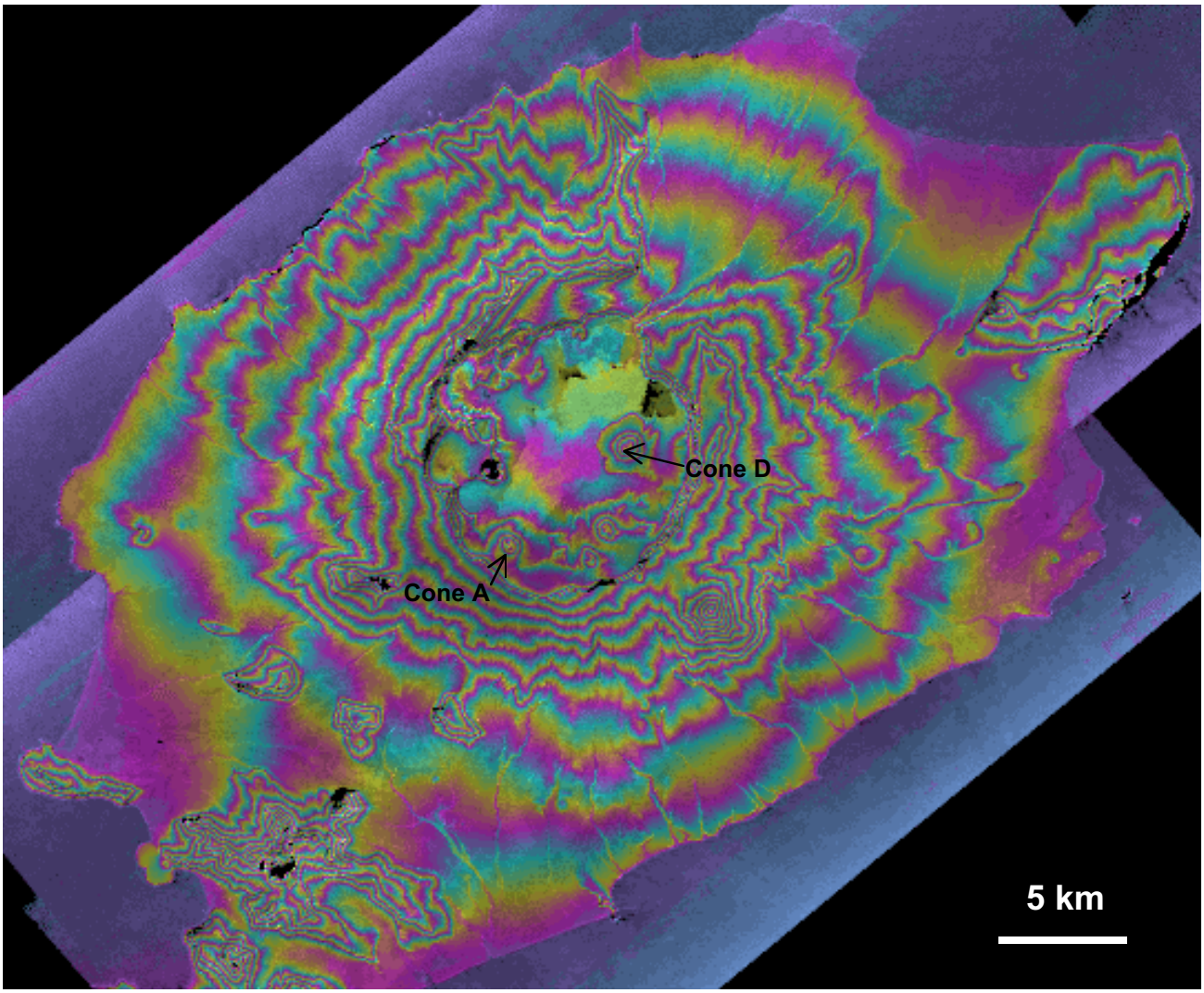

Figure 1. Post-eruption DEM over the Okmok volcano, Alaska using TOPSAR DEMs. Three dimensional multi-affined transformation is applied to correct geometric mis-alignment between different passes with overlap. A full cycle of colors represents 100 m of topographic relief.

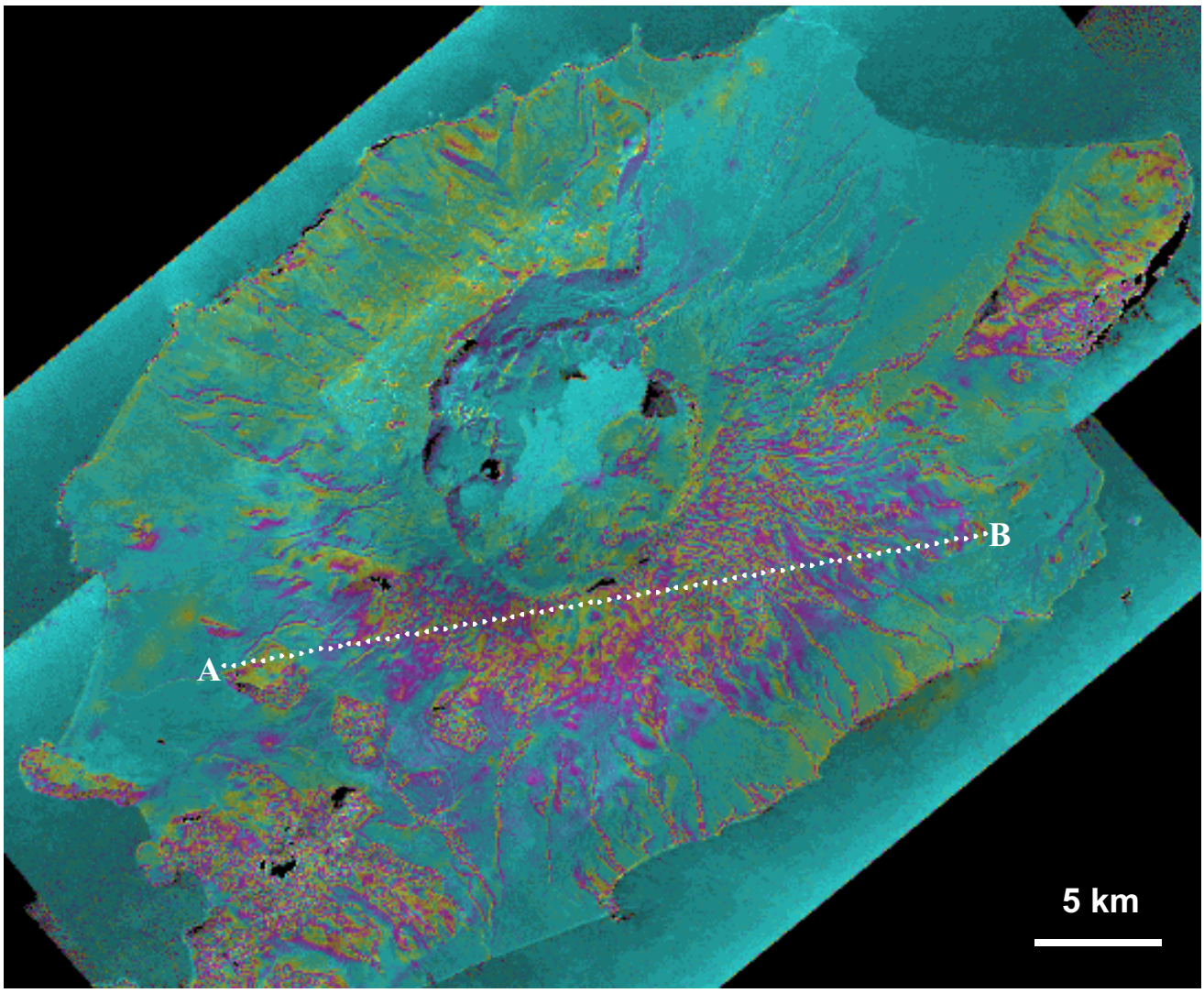

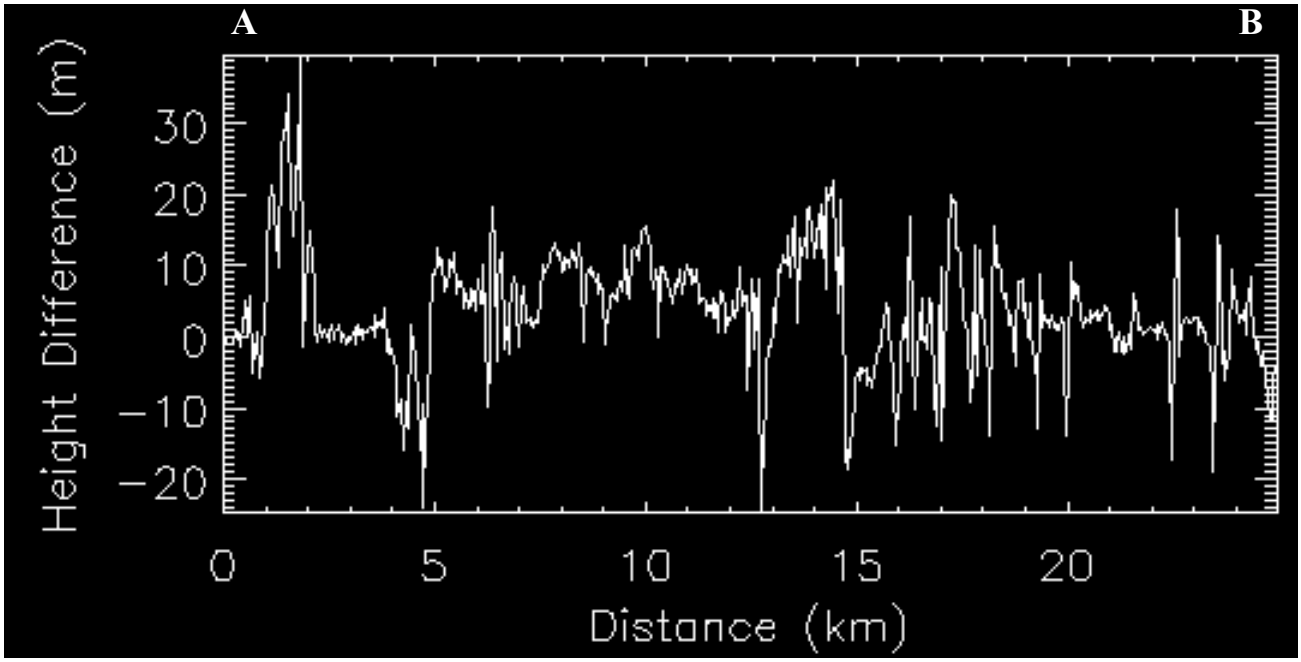

Figure 2. (a) Difference between two DEM mosaics produced with and without geometric correction. A full cycle of colors represents height difference of 15 m. (b) Height difference along a profile from A to B. Height difference ranging from –25 m to 40 m is due to the misalignment in the DEM mosaic

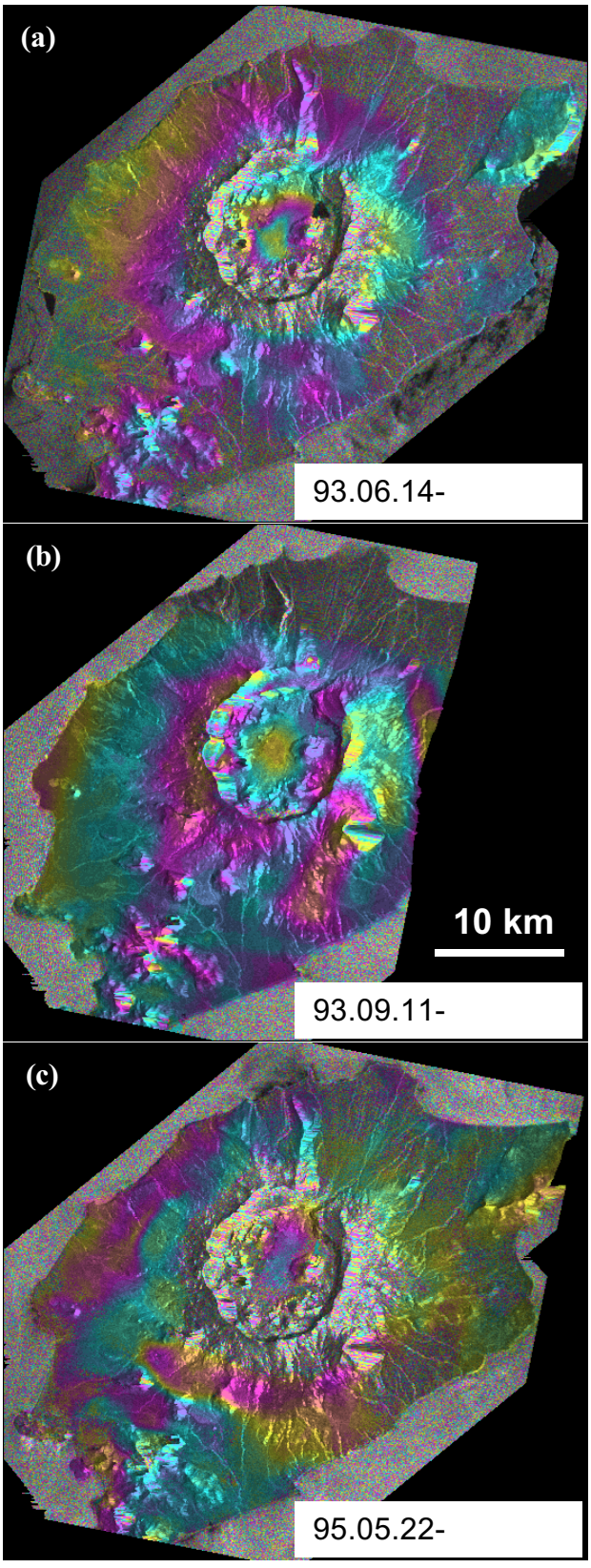

Figure 3. Deformation interferograms during different time periods. The inflation was calculated and removed from those interferograms used for DEM generation. A full cycle of colors represents 28.3 mm surface deformation along the satellite look direction.

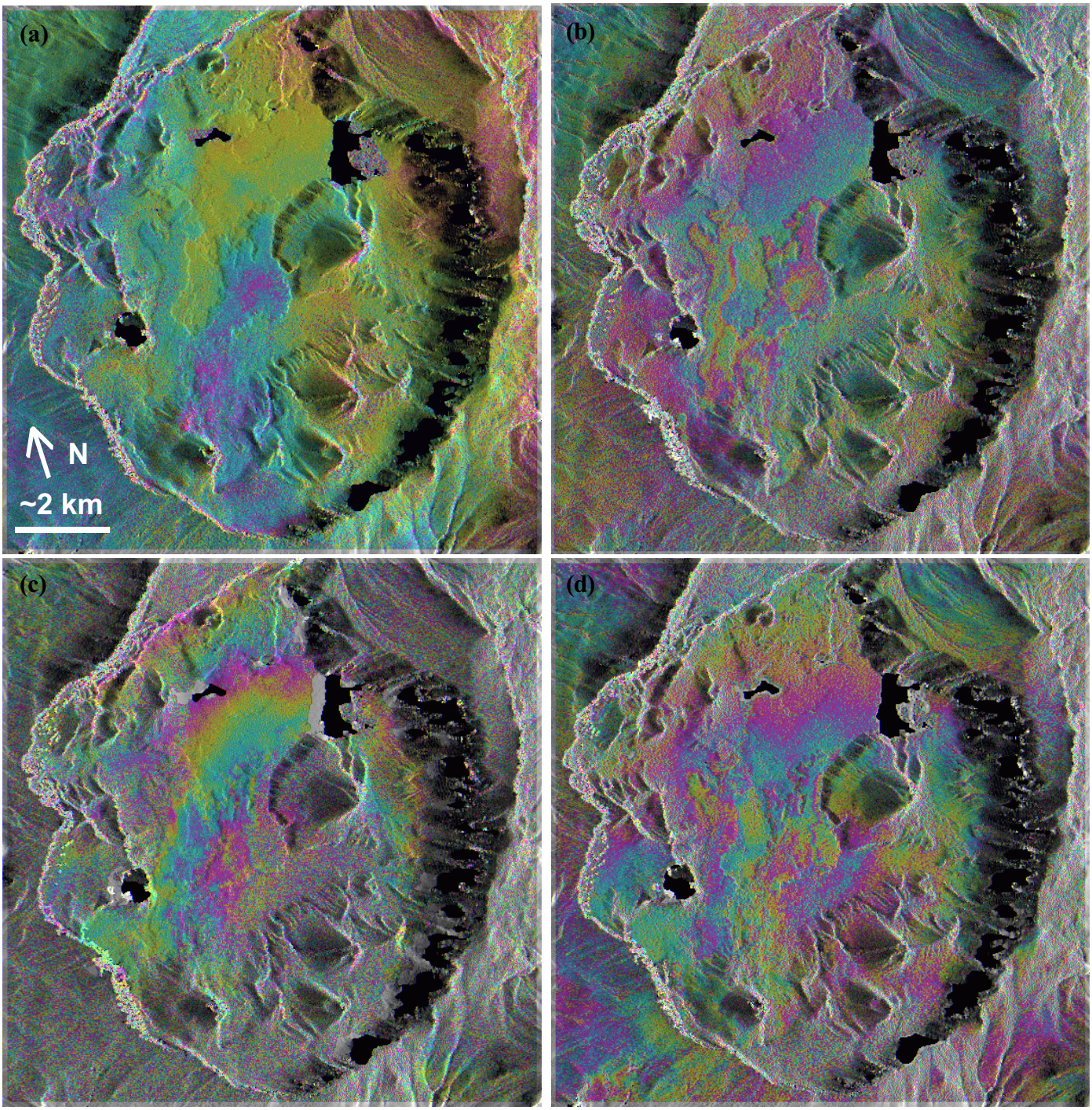

Figure 4. Residual interferograms produced by subtracting topographic phase from the original interferograms (Table 1). (a) The tandem interferogram and the TOPSAR DEM is used to remove the topographic phase. (b) The interferogram with B_n = 403 m and the TOPSAR DEM is used to remove the topographic phase. (c) The interferogram with B_n = 395 m and the DEM produced from the interferogram with B_n = 403 m is used to remove the topographic phase. (d) The interferogram with B_n = 690 m and the DEM produced from the interferogram with B_n = 403 m is used to remove the topographic phase. A full cycle of colors represents a phase change of 360 degrees.

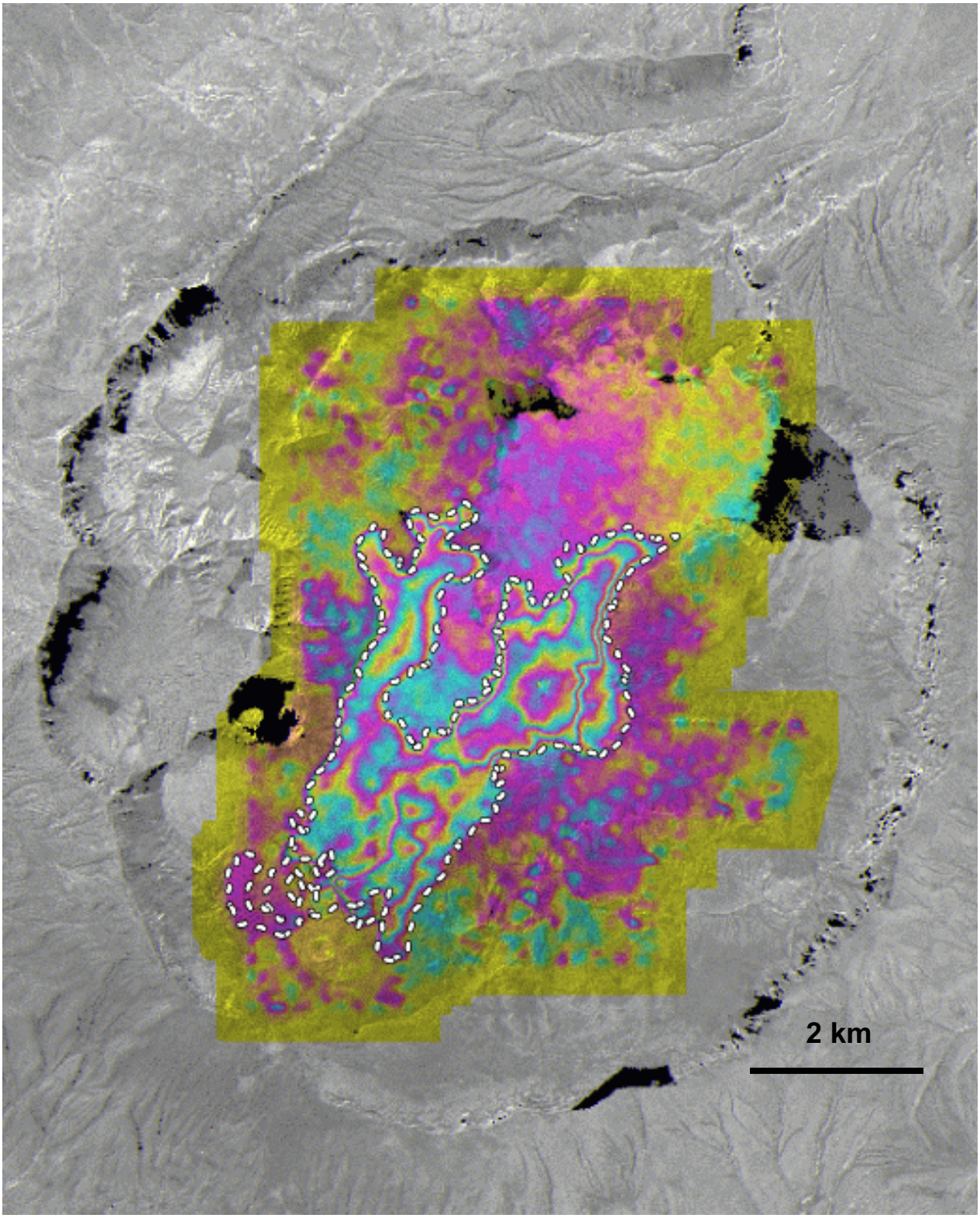

Figure 5. Thickness of lava flows for April 1997 eruption at Okmok volcano. The thickness is derived based on height difference between the pre-eruption and post-eruption DEMs. A full cycle of colors represents lava thickness of 15 m.

Table 1. Interferometric Data Acquisition Parameters

Orbit 1	Orbit 2	Date 1	Date 2	*Bn* (m)
E1_22376	E2_02703	19951025	19950126	83
E1_10781	E1_22282	19930807	19930911	403
E1_11783	E1_12284	19931016	19931120	395
E1_11010	E1_11511	19930823	19930927	690